Optimization of Picrosirius Red Staining Protocol to Determine Collagen Fiber Orientations in Vaginal and Uterine Cervical Tissues by Mueller Polarized Microscopy

ANDRÉ NAZAC,[1,4]* STÉPHANE BANCELIN,[2] BENJAMIN TEIG,[3] BICHER HAJ IBRAHIM,[4] HERVÉ FERNANDEZ,[1,5] MARIE-CLAIRE SCHANNE-KLEIN,[2] AND ANTONELLO DE MARTINO[4]
[1]*Department of Gynecology and Obstetrics, Bicêtre Hospital, Le Kremlin Bicêtre, France*
[2]*Laboratoire D'optique Et Biosciences, Ecole Polytechnique, CNRS, INSERM U696, Palaiseau, 91128, France*
[3]*Department of Anatomopathology, Bicêtre Hospital, Le Kremlin Bicêtre, France*
[4]*Laboratoire De Physique Des Interfaces Et Des Couches Minces (LPICM), Ecole Polytechnique, CNRS, Palaiseau, 91128, France*
[5]*Paris XI University, Orsay, France*

KEY WORDS polarized microscopy; multiphoton microscopy; connective tissue; histological staining; collagen; Mueller polarimetry

ABSTRACT Polarized microscopy provides unique information on anisotropic samples. In its most complete implementation, namely Mueller microscopy, this technique is well suited for the visualization of fibrillar proteins orientations, with collagen in the first place. However, the intrinsic optical anisotropy of unstained tissues has to be enhanced by Picrosirius Red (PR) staining to enable Mueller measurements. In this work, we compared the orientation mapping provided by Mueller and second harmonic generation (SHG) microscopies on PR stained samples of vaginal and uterine cervix tissues. SHG is a multiphoton technique that is highly specific to fibrillar collagen, and was taken as the "gold standard" for its visualization. We showed that Mueller microscopy can be safely used to determine collagen orientation in PR stained cervical tissue. In contrast, in vaginal samples, Mueller microscopy revealed orientations not only of collagen but also of other anisotropic structures. Thus PR is not fully specific to collagen, which necessitates comparison to SHG microscopy in every type of tissue. In addition to this study of PR specificity, we determined the optimal values of the staining parameters. We found that staining times of 5 min, and sample thicknesses of 5 μm were sufficient in cervical and vaginal tissues. *Microsc. Res. Tech. 78:723–730, 2015.* © 2015 Wiley Periodicals, Inc.

INTRODUCTION

Collagen fibers are key structural proteins in the architecture of tissues (Hulmes, 2002; Parry and Craig, 1984). Alteration of collagen organization is strongly connected to various pathologies, including vaginal prolapses (Jackson et al., 1996; Norton et al., 1992) or cervical neoplasias in gynecology (Arifler et al., 2007; Das et al., 2013; Shukla and Pradhan, 2009). Visualization of collagen structures by pathologists is therefore a great concern.

Picrosirius red (PR) has been reported decades ago to stain connective tissues (Sweat et al., 1964). The pioneering study by Junqueira et al. (1979) suggested that PR staining combined with polarized microscopy detects collagen fibers with high specificity. When applied to a tissue, Sirius Red molecules indeed align along collagen fibers, and enhance the birefringence of these anisotropic structures, which in turn provides a specific contrast with polarized microscopy. Detailed staining protocols have been described in various tissues, including vagina, but not uterine cervix. In the former tissue, 1-h PR staining was reported to be the most efficient method to specifically visualize collagen using polarized microscopy (Borges et al., 2007).

While other staining techniques, such as Masson's trichrome, are routinely used by pathologists, they do not provide enough specificity to collagen fibers in connective tissues. In contrast, immunohistochemical staining probes a particular collagen type with great specificity, for instance type I collagen, the prominent fibrillar collagen. Nevertheless, this technique is somewhat delicate and costly compared to histological staining, so that it is not used at all times by pathologists in routine diagnoses (Jeffrey and Prichard., 2014).

Advanced imaging techniques with three-dimensional capabilities have also been reported for collagen visualization. While optical coherence tomography or reflectance confocal microscopy may lack specificity or sensitivity to collagen fibers, second harmonic generation microscopy (SHG) has been shown to

*Correspondence to: A. Nazac; Department of Gynecology, Bicêtre Hospital, 78 Rue General Leclerc, 94270 Le Kremlin Bicêtre, France. E-mail: andre.nazac@bct.aphp.fr

Received 21 January 2015; accepted in revised form 14 May 2015

REVIEW EDITOR: Prof. Alberto Diaspro

Contract grant sponsor: INCa (French Institute of Cancer) via the PAIR-Gynéco project.

DOI 10.1002/jemt.22530
Published online 12 June 2015 in Wiley Online Library (wileyonlinelibrary.com).

© 2015 WILEY PERIODICALS, INC.

probe collagen fibers in intact tissues with high specificity and sensitivity (Campagnola et al., 2002; Cox et al., 2003; Strupler et al., 2007; Zipfel et al., 2003). This method, a multiphoton imaging technique based on a femtosecond infrared laser, is however complex and expensive and has not been used by pathologists in routine diagnosis so far. Note that SHG setups can simultaneously provide two photon excited fluorescence (2PEF) images. This latter imaging modality allows the visualization of other components than collagen in unstained tissues, such as elastin or various cellular chromophores (Zipfel et al., 2003).

The aim of this paper is to optimize PR staining protocols for polarized microscopy in its most complete implementation, i.e. Mueller microscopy. Here we briefly describe the essentials of the technique but the reader interested in the details of this technique will find complete information in references (Bancelin et al., 2014; Laude-Boulesteix et al., 2004). While standard polarized microscopy consists in placing the sample between two crossed linear polarizers, or two opposite sense circular polarizers, in Mueller microscopy the sample is illuminated via a polarization state generator, which sequentially generates four different polarization states, and the emerging light is analyzed by a polarization state analyzer, which generates four different polarization filters. As a result, Mueller microscopy provides a full characterization of the polarimetric response of the sample. In particular, anisotropic samples exhibit an orientation-dependent refractive index, with high and low index axes (also called slow and fast axes), 90° apart from each other. This optical anisotropy introduces a difference in the optical path, also called retardation and expressed in degree or radian, between the polarizations aligned with the slow and fast axes. The value of the retardation (also called scalar retardation) is related to the sample birefringence and considered as a measurement of the sample anisotropy. While standard polarized microscopy can only provide qualitative information about the sample optical anisotropy, Mueller polarimetry provides a measure of the scalar retardation and the orientation (azimuthal angle) of slow and fast axes at each point of the image.

Interestingly, when fibrillar proteins are present in a tissue with a preferential orientation, they induce an optical anisotropy, with the slow axis aligned with the fibers (Junqueira et al., 1979; Wolman and Kasten, 1986). In this context, Mueller polarimetry may provide a reliable, simple and low-cost method to visualize collagen fiber organization in vaginal and uterine cervix, and probably many other human tissues. To validate this idea, we compared Mueller images of PR stained histological sections to SHG images of the same sections as "gold standard" references for collagen fiber visualization. 2PEF images have also been used to improve the visualization of the tissue morphology. In this work, we focused on the organization of collagen fibers lying under Malpighian epithelium in uterine cervix because we expect this organization to be altered in neoplastic tissues with respect to healthy ones to account for the polarimetric responses observed in macroscopic images of conizations (Pierangelo et al., 2013). We also probed collagen distribution in vaginal biopsies because it may be altered with prolapse, a frequent pathology with unknown etiology (Badiou et al., 2008; Kerkhof et al., 2009).

MATERIALS AND METHODS

Tissue Preparation

Five vaginal samples were collected from patients either operated for a grade three vaginal prolapse (Visco et al., 2003) (3 females) or for a hysterectomy for functional reasons (2 females) after obtaining their consent. These samples were removed from the anterior vagina wall, up to two centimeters on a median line from the uterine cervix to the proximal direction. These samples were 2 cm long and 0.5 cm wide, on the entire vaginal thickness from the epithelium to the adventitia. Eleven uterine cervical cones were also collected from patients after obtaining their consent, including 10 conizations performed because of grade 3 cervical intraepithelial neoplasia (CIN3) and 1 conization sampled during hysterectomy due for menorrhagia. Note that the collagen distribution of these vaginal and uterine samples may be affected by the underlying pathology. This advantageously provides different types of samples for comparison of Mueller and SHG imaging.

Each sample was processed to obtain histological sections using the usual protocol of standard microscopy, summarized in Figure 1. The epithelium was marked with black ink, and samples were fixed in neutral formalin for 24–48 h and embedded in paraffin. Sections were cut from each paraffin block and stained with Picrosirius red for collagen visualization or Hematoxylin, Eosin and Safran (HES) for usual histological diagnosis. Finally, each histological section was positioned on a glass slide and covered by a glass cover slip instead of the usual plastic film to avoid birefringence artefacts due to this anisotropic plastic film.

Two parameters were tested in PR stained sections. First, these sections were cut to three different thicknesses: 5 μm (which corresponds to the usual section thickness for histological diagnoses), 10 and 15 μm to take advantage of SHG three-dimensional imaging in thick tissues. Second, slides were incubated with PR over 5–60 min, the latter duration corresponding to optimized protocols as reported for vaginal tissues (Borges et al., 2007). Table 1 summarizes the main features of the tissues under study and the number of measures with Mueller polarimetric and second harmonic generation microscopies.

Comparative Study of Mueller and SHG Imaging

Each section was imaged using polarization and multiphoton microscopies in the same regions for the sake of comparison. To that end, 1×1 mm^2 areas were delineated on the glass coverslip using black ink as shown in Figure 1. Polarization images were then recorded within these delineated areas in regions of interests (ROIs) exhibiting remarkable patterns to facilitate image registration (480×480 μm^2 field of view). Finally, SHG imaging was performed in the very same ROIs by adjusting the section position in the microscope stage until visualizing similar patterns on the multiphoton images. 2PEF images were recorded simultaneously to better reveal the tissue morphology through endogenous fluorescent signals

10970029, 2015, 8, Downloaded from https://analyticalsciencejournals.onlinelibrary.wiley.com/doi/10.1002/jemt.22530 by Universite De Bordeaux, Wiley Online Library on [11/04/2025]. See the Terms and Conditions (https://onlinelibrary.wiley.com/terms-and-conditions) on Wiley Online Library for rules of use; OA articles are governed by the applicable Creative Commons License

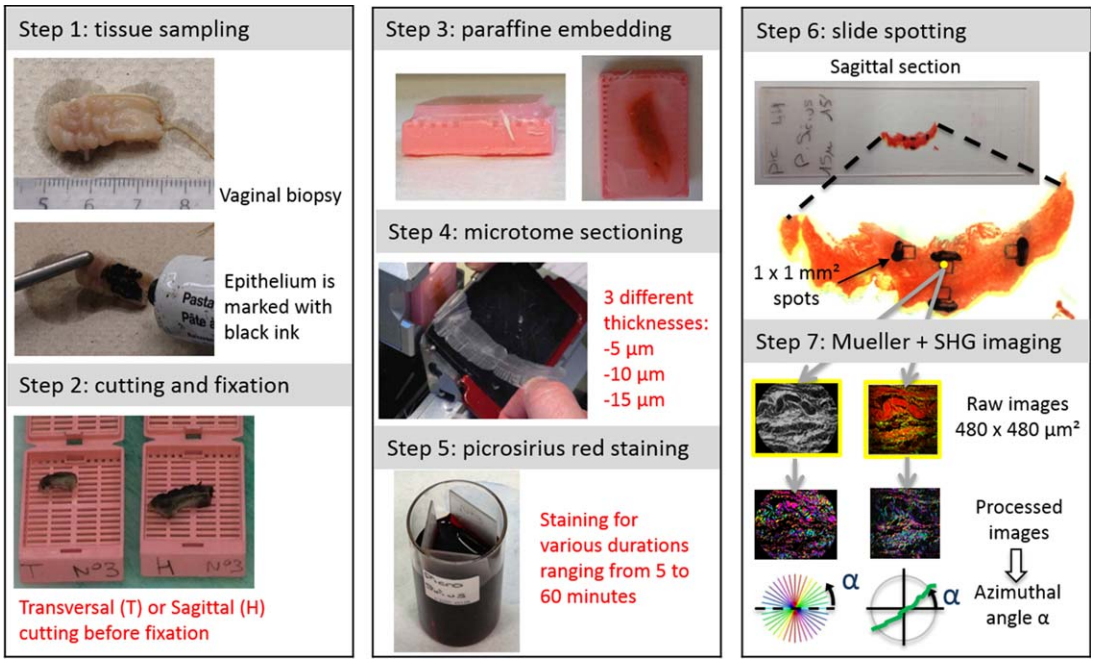


Fig. 1. Essential steps (1–5) of the pathology procedure providing histological slides from a fresh tissue biopsy. In step 6, these slides are marked to delineate areas (open squares in the zoom at the bottom of the figure) within which identical ROIs were identified and imaged by both multiphoton and Mueller microscopies (step 7). [Color figure can be viewed in the online issue, which is available at wileyonlinelibrary.com.]

TABLE 1. Summary of the tissue samples studied with Mueller polarimetry (MP) and second harmonic generation (SHG) microscopy

Tissue	Patient	Clinical indication	Mueller polarimetry	Second harmonic generation
Vaginal tissue	V1	Grade 3 vaginal prolapse	Yes (80 images/13 slides)	Yes (27 images/6 slides)
	V2	Grade 3 vaginal prolapse	Yes (44 images/6 slides)	No
	V3	Grade 3 vaginal prolapse	Yes (4 images/1 slide)	No
	V4	Hysterectomy for functional reasons	Yes (12 images/12 slides)	No
	V5	Hysterectomy for functional reasons	Yes (12 images/12 slides)	No
Uterine cervix	C1	CIN3	Yes (12 images/1 slide)	Yes (6 images/1 slide)
	C2	CIN3	Yes (28 images/1 slide)	Yes (9 images/1 slide)
	C3	CIN3	Yes (17 images/1 slide)	No
	C4	CIN3	Yes (10 images/1 slide)	No
	C5	CIN3	Yes (11 images/1 slide)	No
	C6	CIN3	Yes (7 images/1 slide)	No
	C7	CIN3	Yes (9 images/1 slide)	No
	C8	CIN3	Yes (7 images/1 slide)	No
	C9	CIN3	Yes (6 images/1 slide)	No
	C10	CIN3	Yes (7 images/1 slide)	No
	C11	Hysterectomy due to menorrhagia	Yes (6 images/1 slide)	No

(enhanced by the fixation process) and facilitate comparison with polarization images.

In vaginal sections, we delineated 1×1 mm^2 areas in the three layers of the vaginal wall namely the submucosa, the muscularis and the adventitia (Boreham et al., 2002; Weber and Walters, 1997). We then imaged with Mueller microscopy a total of 152 ROIs in 44 slides with different thickness or staining duration from the 5 patients (see Table 1). 27 ROIs in 6 slides from 1 patient were also imaged with SHG microscopy. In cervical sections, we focused on subepithelial regions corresponding to two different epithelial states, either healthy Malpighian epithelium or CIN3. We then imaged using Mueller microscopy a total of 120 ROIs (just under the epithelial layer) in 11 slides from the 11 patients (6 to 28 images per slide, see Table 1). 15 ROIs in 2 slides from 2 patients (6–9 images per slide) were also imaged using SHG microscopy.

Mueller and SHG images were then processed as previously published (Bancelin et al., 2014). Briefly, complete Muller measurements provided azimuthal (in plane) angular orientation of the slow optical axis of the PR-enhanced retardation. SHG images provided a direct visualization of the collagen fibers, whose azimuthal orientation was obtained directly from the images after suitable filtering. The azimuthal angles obtained by Mueller and SHG techniques were directly compared on processed images of the same ROIs using the same RGBR color code (red to green to blue to red again from 0° to 180°). Further processing provided the corresponding histograms of the azimuthal angles of all pixels of every ROI.

10970029, 2015, 8, Downloaded from https://analyticalsciencejournals.onlinelibrary.wiley.com/doi/10.1002/jemt.22530 by Universite De Bordeaux, Wiley Online Library on [11/04/2025]. See the Terms and Conditions (https://onlinelibrary.wiley.com/terms-and-conditions) on Wiley Online Library for rules of use; OA articles are governed by the applicable Creative Commons License

Influence of Section Thickness and Staining Duration for Mueller Microscopy

In order to optimize PR staining duration for Mueller microscopy, we measured the mean scalar retardation on the full field of view as a function of the staining duration. This study was performed on vaginal sections because they are more homogenous than cervical sections. Staining durations were 5, 10, 15, 30, and 60 min. We also imaged unstained vaginal sections to test the intrinsic retardation of these samples.

In order to verify the consistency of our measurements, we imaged four sets of vaginal serial sections (15 min Picrosirius red staining) with three different thicknesses: 5, 10, and 15 μm. We then compared the mean scalar retardations over the full field of view.

RESULTS

Comparative Study of Mueller and SHG Imaging of Vaginal Tissue

Figure 2 displays typical results obtained from Mueller and multiphoton microscopies in the same ROI of a vaginal sagittal section, in the muscularis layer (patient V1). The unpolarized transmitted light (Fig. 2A) and SHG (green color in Fig. 2B) images exhibit similar structures in some regions but not everywhere in the field of view. All the structures revealed by the SHG image also appear in the transmitted light image, while, in contrast, some structures in the transmitted light images are not present in the SHG image, but appear in the 2PEF image (red color in Fig. 2B). The white circle identifies one spot exhibiting such behavior in images 2A–2D). The orientation images (Figs. 2C and 2D) obtained from both SHG and Mueller imaging techniques also show similar azimuthal angles in some regions but not everywhere, and in particular not in the above-mentioned SHG-silent regions. Finally, the orientation histograms (Figs. 2E and 2F) do not match, which confirms that only a minor pixel number in Mueller and SHG images show similar orientations.

Comparative Study of Mueller and SHG Imaging of Cervical Tissue

Figure 3 displays typical orientation images obtained from polarization and multiphoton microscopies in the same ROI of a cervical section, around a crypt in a healthy region (patient C1), which corresponds to an invagination of the glandular epithelium into the substance of the cervical stroma. The unpolarized transmitted light image (Fig. 3A) and the raw SHG image (Fig. 3B) exhibit similar structures in the whole field of view. Interestingly, both images show that the residual mucus present in the crypt lumen is slightly stained by PR and appears in the 2PEF image but not in the SHG one. The orientation images (Figs. 3C and 3D) and the histograms (Figs. 3E and 3F) obtained from the two techniques also match in a satisfactorily way.

Influence of Section Thickness for Mueller Imaging

Table 2 displays the mean scalar retardation for serial vaginal sections with the same staining duration (15 min) as a function of the section thickness. We observe no strong variation within the range under study, while scalar retardation is expected to increase linearly with sample thickness in homogeneous samples.

Optimization of Picrosirius Red Staining Duration for Mueller Imaging

Originally, we studied unstained vaginal sections to verify whether the intrinsic collagen retardation may be measured using polarization microscopy. We observed no significant signal even in 15 μm thick sections on 30 different slides. On these slides, the mean scalar retardation is only 2°, which corresponds to the background noise measured in the polarization microscope.

The effect of the staining duration was studied by plotting histograms of the scalar retardation for various staining durations. A typical result is shown in Figure 4 for serial vaginal sections (patient V4). When the staining time increases, the histogram gets wider, implying a significant increase of the mean value with respect to the 2° measured without staining. Table 3 displays the mean scalar retardation for serial sections showing similar histological structures. These sections are either sagittal or transversal sections with the same thickness (15 μm) from five different patients. We did not observe any differences in the mean retardation of sagittal or transversal sections and merged the results of both types of sections. Table 3 shows that different samples with the same staining duration exhibit similar mean scalar retardations.

DISCUSSION

Comparative Study of Mueller and SHG Imaging of Vaginal Tissue

Considering that SHG specifically reveals collagen fibers and that the transmitted light MP image reveals absorption by Picrosirius red, we deduce that the transmitted light image shows some absorbing components that are not collagen fibers and still are stained by Picrosirius red and appear in 2PEF images. The nonzero retardance observed in most of these regions indicates that the PR molecules exhibit local preferential orientations, which certainly highlight the local preferential orientations of the components other than collagen visualized by 2PEF. Similar observations have been reported in other tissues, and it has been suggested that these oriented PR stained components may be oriented basic proteins or amyloid fibrils (Constantine and Mowry, 1968; Junqueira et al., 1979). While the accurate nature of these components is beyond the aim of this study, our data clearly show that MP of PR stained vaginal tissue is not fully specific for collagen.

Comparative Study of Mueller and SHG Imaging of Cervical Tissue

The residual mucus present in the crypt lumen is composed of biomolecules other than collagen, which explains the absence of any SHG signal. It is nevertheless slightly stained by PR, but no significant scalar retardation is seen in the MP image, which means that the PR molecules do not exhibit any preferential orientation, even at the micrometer scale. This complete

10970029, 2015, 8, Downloaded from https://analyticalsciencejournals.onlinelibrary.wiley.com/doi/10.1002/jemt.22530 by Universite De Bordeaux, Wiley Online Library on [11/04/2025]. See the Terms and Conditions (https://onlinelibrary.wiley.com/terms-and-conditions) on Wiley Online Library for rules of use; OA articles are governed by the applicable Creative Commons License

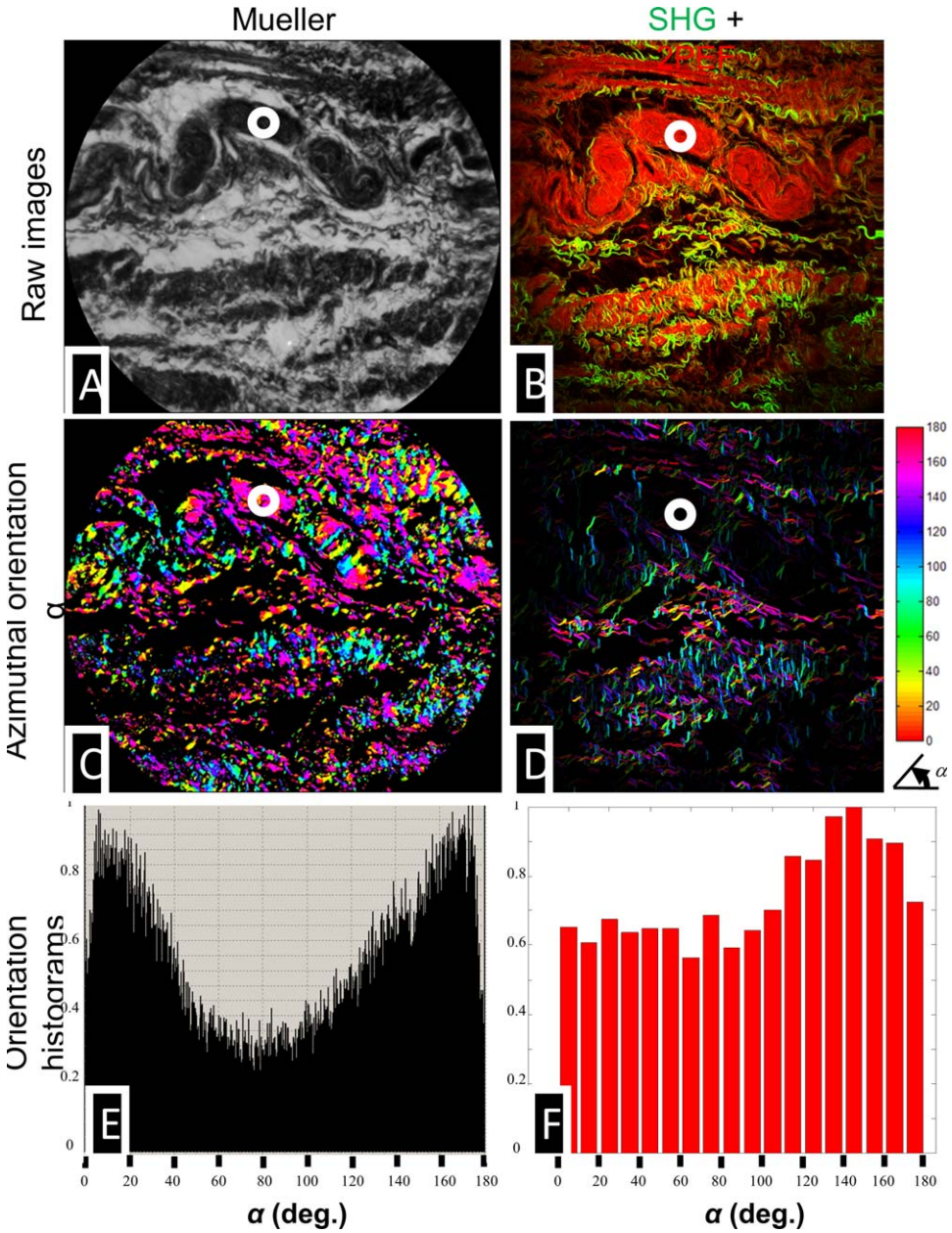


Fig. 2. Comparison of Mueller and combined SHG/2PEF microscopies on the same region of a vaginal sample. (**A**) Unpolarized transmitted light image at 550 nm. Transmission varies from 0 (black) to 1 (white). (**B**) Multiphoton image upon 860 nm excitation, where SHG (in green) shows collagen fibers and 2PEF (in red) other tissue components. (**C**) Azimuthal orientation a of the retardation slow axis, displayed in the RGBR scale from 0° to 180° shown on the right side. (**D**) Azimuthal orientation of the collagen fibers derived from the SHG image. (**E**) Histogram of the slow axis orientation. (**F**) Histogram of the collagen fibers orientation. The white circle highlights a region without collagen but with 2PEF active biomolecules (image b). This region exhibits significant retardance with well defined orientation of slow axis (image c). Images size: 480 × 480 μm^2. [Color figure can be viewed in the online issue, which is available at wileyonlinelibrary.com.]

orientational disorder of the PR molecules is attributed to a similar disorder of the components the PR molecules stick on.

Orientation histograms measured from both techniques are in good agreement. They exhibit the same shape with a main peak corresponding to the major azimuthal orientation in the image. While the width and the contrast of the peaks are different for the two techniques, due to various filtering techniques, both histograms peak at the same angle, so that they provide the same main orientation of collagen fibers. The peaks of the orientation histograms provided by the two techniques have been found to coincide to within 7° (rms) in a study on 12 different samples of cervical tissue. More details about this study have been published recently in the reference (Bancelin et al., 2014).

10970029, 2015, 8, Downloaded from https://analyticalsciencejournals.onlinelibrary.wiley.com/doi/10.1002/jemt.22530 by Universite De Bordeaux, Wiley Online Library on [11/04/2025]. See the Terms and Conditions (https://onlinelibrary.wiley.com/terms-and-conditions) on Wiley Online Library for rules of use; OA articles are governed by the applicable Creative Commons License

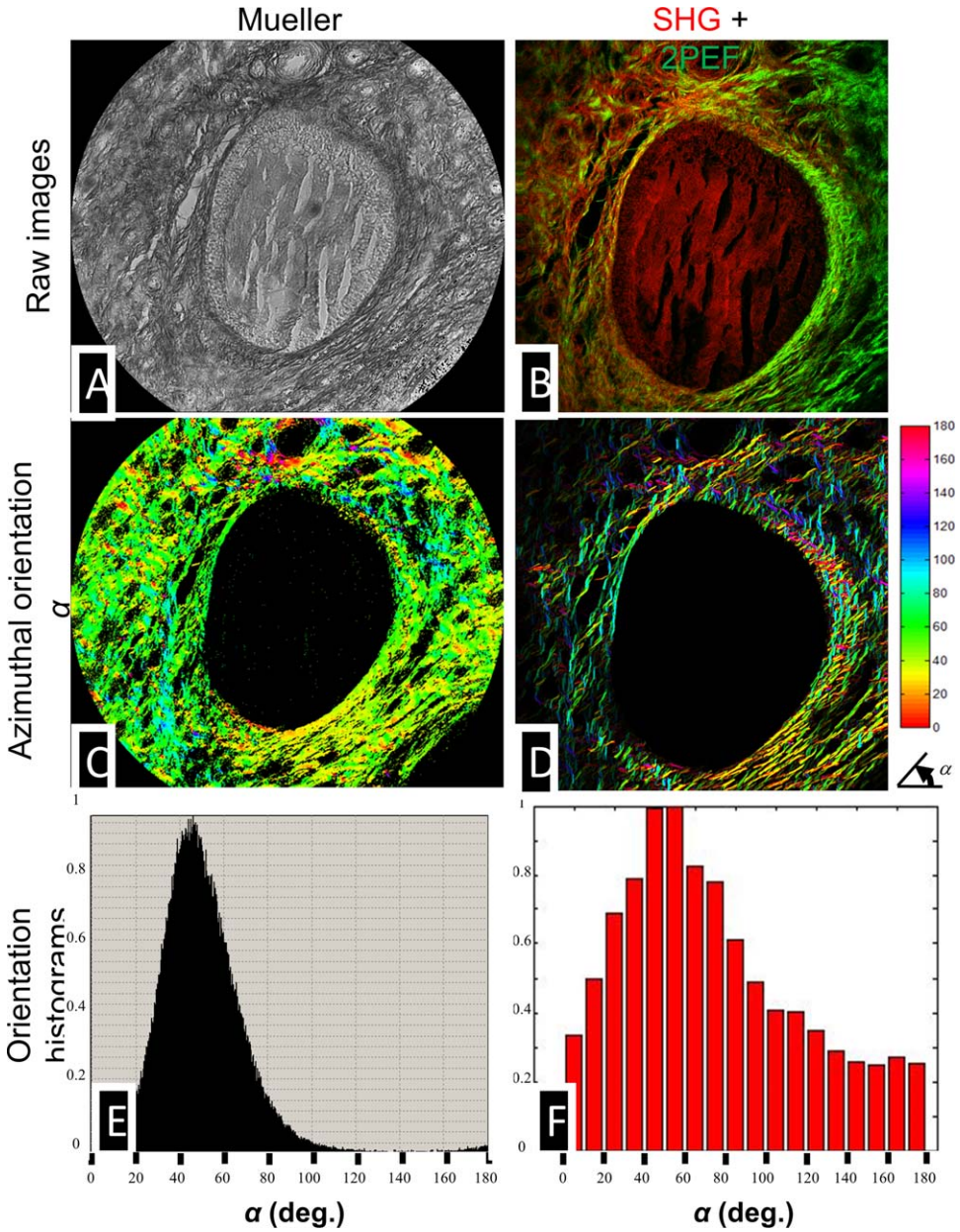


Fig. 3. A-F: Analogs to Figure 2, for a histological section of healthy uterine cervical tissue beneath the epithelium with a crypt. This crypt is partially filled with mucus, which is clearly visible in transmission and 2PEF images (**A** and **B**). Images size: 480 × 480 μm^2. [Color figure can be viewed in the online issue, which is available at wileyonlinelibrary.com.]

These results show that in PR stained cervical tissue, Mueller microscopy based on scalar retardation measurements only reveals collagen fibers.

Influence of Section Thickness for Mueller Imaging

The absence of any increase of scalar retardation with sample thickness may be attributed to sample heterogeneities occurring within the section, leading to variations of the collagen density and organization along the section thickness. As a consequence, increasing the section thickness is not effective to enhance the scalar retardation and 5–10 μm are sufficient to optimize the retardation for these samples.

Optimization of Picrosirius Red Staining Duration for Mueller Imaging

Mueller imaging of unstained vaginal sections shows that PR staining is mandatory to enhance the collagen retardation and allow detection of these anisotropic structures by polarization microscopy.

Mean scalar retardations of different samples with the same staining duration are in good agreement, although these measurements are performed in tissues

10970029, 2015, 8, Downloaded from https://analyticalsciencejournals.onlinelibrary.wiley.com/doi/10.1002/jemt.22530 by Universite De Bordeaux, Wiley Online Library on [11/04/2025]. See the Terms and Conditions (https://onlinelibrary.wiley.com/terms-and-conditions) on Wiley Online Library for rules of use; OA articles are governed by the applicable Creative Commons License

TABLE 2. Mean scalar retardation (degree) as a function of section thickness (μm) in serial vaginal sections stained for 15 min from patients V4 and V5 (transversal and sagittal sections)

Patient number	Histological region	Mean scalar retardation for various staining durations				
		5 min	10 min	15 min	30 min	60 min
C1	Adventitia	5.4 ± 0.8 (n = 6)	6.0 ± 1.0 (n = 6)	7.0 ± 1.1 (n = 23)	NA	NA
C1	Muscularis	5.9 ± 0.8 (n = 2)	NA	8.6 ± 1.3 (n = 20)	NA	NA
C1	Submucosa	7.5 ± 2.6 (n = 2)	5.6 (n = 1)	8.9 ± 1.7 (n = 20)	NA	NA
C2	Adventitia	7.4 ± 1.2 (n = 13)	NA	NA	NA	NA
C2	Muscularis	6.8 ± 1.9 (n = 15)	NA	NA	NA	NA
C2	Submucosa	5.6 ± 0.7 (n = 16)	NA	NA	NA	NA
C3	Muscularis	NA	NA	9.7 ± 1.6 (n = 4)	NA	NA
C4	Muscularis	NA	NA	9.5 ± 2.0 (n = 2)	12.5 ± 6.4 (n = 2)	13.2 ± 3.7 (n = 2)
C5	Muscularis	NA	NA	12.9 ± 2.3 (n = 2)	11.8 ± 0.1 (n = 2)	13.3 ± 1.1 (n = 2)

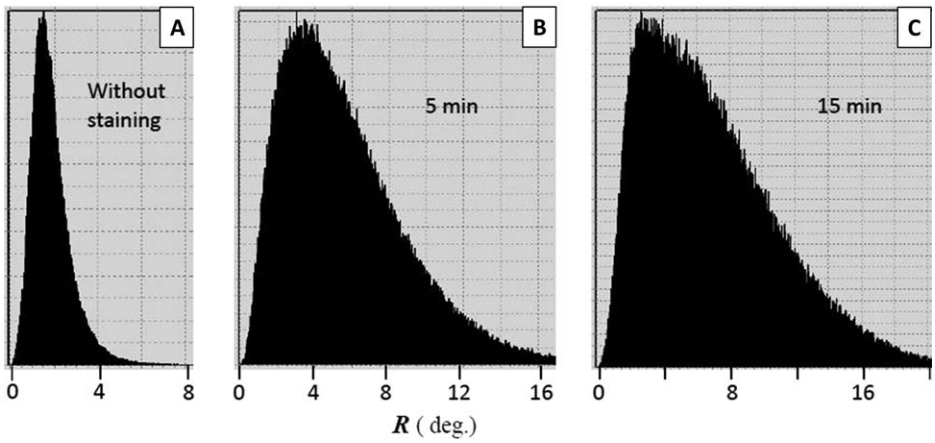


Fig. 4. Histograms of the scalar retardation values measured over the whole field of view for three different staining durations. Sample thickness: 15 μm.

TABLE 3. Mean scalar retardation (degree) for various staining duration (min) in 152 ROIs from different sagittal or transversal vaginal sections from five patients

Sample	Thickness (μm)		
	5	10	15
V4H	9.5	13	10.9
V4T	8.4	13.9	8
V5H	20.7	10.9	11.3
V5T	9.7	11.3	14.5

Sections from the same sample are 15 μm thick serial sections. NA stands for Not Available (no section imaged).

with complex collagen distribution instead of "model" tissues, such as rat tendons exhibiting highly uniform density and orientation of collagen fibers. Accordingly, we observe a significant variability in the retardation values, due to significant dispersion of collagen density and polar angles (which are not currently accessible in Mueller microscopy). Nevertheless, Table 3 shows unambiguously the reproducibility of Mueller measurements.

We also consistently observe that the mean scalar retardation increases with the staining duration, but in a sublinear way. It may be attributed to a faster tissue staining at the beginning of the procedure, followed by progressive saturation of the stain access to collagen fibers. Most importantly, the scalar retardation measured for only 5 min staining is significantly higher than the background noise level and therefore enables the azimuthal angle measurement in a reliable way.

In conclusion, this study was devoted to the use of Mueller polarized microscopy of Picrosirius red stained samples for the visualization of collagen fiber orientations in vaginal and uterine cervical tissues. Our main results are twofold.

First, we compared the data provided by Mueller and multiphoton (SHG and 2PEF) microscopies, SHG being the "gold standard" for collagen fiber visualization. We showed that Mueller microscopy in conjunction with PR staining provides reliable orientation images in cervical tissue, which is known to be rich in collagen, in contrast with vaginal tissue, where these images include contributions from other components which show up in 2PEF images. Thus, PR staining is not totally specific for collagen as suggested by previous studies, and each type of tissue should be investigated by comparison with other techniques, such as SHG microscopy to assess the specificity of PR staining and to correctly interpret the data provided by polarized imaging.

Second, we determined an acceptable "window" for the samples thickness and staining time to obtain

10970029, 2015, 8, Downloaded from https://analyticalsciencejournals.onlinelibrary.wiley.com/doi/10.1002/jemt.22530 by Universite De Bordeaux, Wiley Online Library on [11/04/2025]. See the Terms and Conditions (https://onlinelibrary.wiley.com/terms-and-conditions) on Wiley Online Library for rules of use; OA articles are governed by the applicable Creative Commons License

adequate retardations. With our system, these retardations must be larger than 3° for a sufficient fraction of pixels (of the order of 80%). Such retardations are obtained in cervical and vaginal tissues with 5 min staining duration, which is much shorter than previously published values, and 5 μm thicknesses, which are compatible with standard histological practice. Such an information should be of great interest for pathologists by providing a reliable method for the analysis of the extracellular matrix in histological sections with very low staining duration.

ACKNOWLEDGMENT

We thank Martine Prsle, technician at the Pathology Department of Bicêtre hospital for having kindly prepared all histological slides manually.

REFERENCES

Arifler D, Pavlova I, Gillenwater A, Kortum RR. 2007. Light scattering from collagen fiber networks: Micro-optical properties of normal and neoplastic stroma. J. Biophys 92:3260–3274.

Badiou W, Granier G, Bousquet PJ, Monrozies X, Mares P, Tayrac RD. 2008. Etude histologique de la paroi vaginale antérieure dans le prolapsus génital récidivé. Pelv Perineol 3:81–87.

Bancelin S, Nazac AH, Ibrahim B, Dokladal P, Decencière E, Teig B, Haddad H, Fernandez H, Schanne-Klein MC, De Martino A. 2014. Determination of collagen fiber orientation in histological slides using mueller microscopy and validation by second harmonic generation imaging. Opt Express 22:22561–22574.

Boreham MK, Wai CY, Miller RT, Schaffer JI, Word RA. 2002. Morphometric analysis of smooth muscle in the anterior vaginal wall of women with pelvic organ prolapse. Am J Obstet Gynecol 187:56–63.

Borges LF, Gutierrez PS, Marana HR, Taboga SR. 2007. Picrosirius-polarization staining method as an efficient histopathological tool for collagenolysis detection in vesical prolapse lesions. Micron 38: 580–583.

Campagnola PJ, Millard AC, Terasaki M, Hoppe PE, Malone CJ, Mohler WA. 2002. Three-dimensional high-resolution second-harmonic generation imaging of endogenous structural proteins in biological tissues. Biophys. J 82:493–508.

Constantine VS, Mowry RW. 1968. Selective staining of human dermal collagen. II. The use of picrosirius red F3BA with polarization microscopy. J Invest Dermatol 50:419−423.

Cox G, Kable E, Jones A, Fraser I, Marconi K, Gorrell MD. 2003. 3-dimensional imaging of collagen using second harmonic generation. J Struct Biol 141:53–62.

Das N, Chatterjee S, Soni J, Jagtap J, Pradhan A, Sengupta TK, Panigrahi PK, Vitkin IA, Ghosh N. 2013. Probing multifractality in tissue refractive index: prospects for precancer détection. Opt Lett 38:211–213.

Hulmes DJS. 2002. Building collagen molecules, fibrils, and suprafibrillar structures. J Struct Biol 137:2–10.

Jackson SR, Avery NC, Tarlton JF, Eckford SD, Bailey AJ, Abrams P. 1996. Changes in metabolism of collagen in genitourinary prolapse. Lancet 347:1658–1661.

Prichard JW. 2014. Overview of automated immunohistochemistry. Arch Pathol Lab Med 138:1578–1582.

Junqueira LCU, Bignolas G, Brentani RR. 1979. Picrosirius staining plus polarization microscopy, a specific method for collagen detection in tissue sections. Histochem J 11:447–455.

Kerkhof MH, Hendriks L, Brölmann HAM. 2009. Changes in connective tissue in patients with pelvic organ prolapse: A review of the current literature. Int Urogynecol J 20:461–474.

Laude-Boulesteix B, Martino AD, Drévillon B, Schwartz L. 2004. Mueller polarimetric imaging system with liquid crystals. Appl Opt 43:2824–2832.

Norton PA, Boyd C, Deak S. 1992. Collagen synthesis in women with genital prolapse or stress urinary incontinence. Neururol Urodyn 11:300–301.

Shukla P, Pradhan A. 2009. Mueller decomposition images for cervical tissue: Potential for discriminating normal and dysplastic states. Opt Express 17:1600–1609.

Parry DAD, Craig AS. 1984. Growth and development of collagen fibrils in connective tissue. In: Ruggeri A, Motta PM, editors. Ultrastructure of the connective tissue matrix. Heidelberg: Springer. pp. 34–64.

Pierangelo A, Nazac A, Benali A, Validire P, Cohen H, Novikova T, Ibrahim BH, Manhas S, Fallet C, Antonelli MR, Martino AD. 2013. Polarimetric imaging of uterine cervix: A case study. Opt Express 21:14120–14130.

Strupler M, Pena AM, Hernest M, Tharaux PL, Martin JL, Beaurepaire E, Schanne-Klein MC. 2007. Second harmonic imaging and scoring of collagen in fibrotic tissues. Opt Express 15:4054–4065.

Sweat F, Puchtler H, Rosenthal SI. 1964. Sirius red f3ba as stain for connective tissue. Arch Pathol 78:69–72.

Visco AG, Wei JT, McClure LA, Handa VL, Nygaard IE. 2003. Effects of examination technique modifications on pelvic organ prolapse quantification (pop-q) results. Int Urogynecol J Pelvic Floor Dysfunct 14:136–140.

Weber AM, Walters MD. 1997. Anterior vaginal prolapse: Review of anatomy and techniques of surgical repair. Obstet Gynecol 89:311–318.

Wolman M, Kasten FH. 1986. Polarized light microscopy in the study of the molecular structure of collagen and reticulin. Histochemistry 85:41–49.

Zipfel WR, Williams RM, Christie RA, Nikitin Y, Hyman BT, Webb WW. 2003. Live tissue intrinsic emission microscopy using multiphoton-excited native fluorescence and second harmonic generation. Proc Natl Acad Sci USA 100:7075–7080.

10970029, 2015, 8, Downloaded from https://analyticalsciencejournals.onlinelibrary.wiley.com/doi/10.1002/jemt.22530 by Universite De Bordeaux, Wiley Online Library on [11/04/2025]. See the Terms and Conditions (https://onlinelibrary.wiley.com/terms-and-conditions) on Wiley Online Library for rules of use; OA articles are governed by the applicable Creative Commons License